JOURNAL OF MATERIALS SCIENCE **40** (2005) 2263–2268

Theoretical model of the interfacial reactions between solid iron and liquid zinc-aluminium alloy

M.-L. GIORGI*, J.-B. GUILLOT
École Centrale Paris, Grande Voie des Vignes, 92 295 Châtenay-Malabry cedex, France
E-mail: Marie-lawrence.giorgi@lgpm.ecp.fr

R. NICOLLE
IRSID, Voie Romaine, BP 30320, 57283 Maizières-lès-Metz cedex, France

Steel strip is often coated with a layer of zinc in order to protect it against corrosion. One of the most commonly used coating processes is continuous hot dip galvanizing. In this process, the steel strip is immersed in a molten zinc bath containing small amounts of aluminium (less than 1 wt%).

A model has been developed describing the kinetics of the galvanizing reactions that occur at the steel/liquid zinc interface (dissolution of iron, heterogeneous nucleation and growth of the intermetallic phase designated $Fe_2Al_5Zn_x$).

The model has been validated using experimental data available in the literature for a classical galvanizing treatment that lasts three seconds. © *2005 Springer Science + Business Media, Inc.*

Nomenclature

$a_{crystal}$	Side of the crystals assumed to be in the form of cubes (m)
a_{Fe}, a_{Al}, a_{Zn}	Activities of iron, aluminium and zinc in the supersaturated bath
a_{Fe}^{sat}, a_{Al}^{sat}, a_{Zn}^{sat}	Activities of iron, aluminium and zinc in the saturated bath
c_{Fe}, c_{Al}	Concentrations of iron and aluminium in the bath ($mol \cdot m^{-3}$)
$c_{Fe}^{\circ liq}$, $c_{Al}^{\circ liq}$	Concentrations of iron and aluminium in the liquid phase in equilibrium with $Fe_2Al_5Zn_x$ ($mol \cdot m^{-3}$)
c_{Fe}^{meta}	Concentration of iron in the liquid zinc in metastable equilibrium with pure iron ($mol \cdot m^{-3}$)
D_{Fe}^{comp}	Diffusion coefficient for iron in the compound ($\approx 10^{-14}$ $m^2 \cdot s^{-1}$) [12, 29]
$D_{Fe}^{Zn(L)}$, $D_{Al}^{Zn(L)}$	Diffusion coefficient for iron ($= 9.8 \times 10^{-10}$ $m^2 \cdot s^{-1}$) [29] and aluminium in liquid zinc ($m^2 \cdot s^{-1}$)
h_{diff}	Thickness of the interface layer (m)
I	Nucleation rate ($m^{-2} \cdot s^{-1}$)
k_B	Boltzman's constant (1.38×10^{-23} $J \cdot K^{-1}$)
k_{diss}	Dissolution rate constant ($m \cdot s^{-1}$)
k_{growth}	Rate constant for the growth of $Fe_2Al_5Zn_x$ ($m \cdot s^{-1}$)
k_{nucl}	Nucleation rate constant ($k_{nucl}/\eta = 10^{31}$ $Pa \cdot m^{-2}$) [26, 27]
M_{comp}	Molar weight of $Fe_{x_{Fe}^{comp}}Al_{x_{Fe}^{comp}}Zn_{x_{Fe}^{comp}}$ (39×10^{-3} $kg \cdot mol^{-1}$)
n_{nucl}	Number of moles of compound per unit surface area contained in the nuclei ($mol \cdot m^{-2}$)
N_{nuclei}	Total number of nuclei per unit surface area ($\approx 4 \times 10^{14}$ m^{-2}) [12]
r_{mean}^{*}	Mean critical radius of the hemispherical embryos (m)
T	Temperature (K)
t	Galvanizing time (s)
t_{nucl}	Time when nucleation begins (s)
V_m	Volume of a molecule of $Fe_{x_{Fe}^{comp}}Al_{x_{Fe}^{comp}}Zn_{x_{Fe}^{comp}}$ ($\approx 1.374 \times 10^{-29}$ m^3) [12, 31]
x_{Fe}^{comp}, x_{Al}^{comp}, x_{Zn}^{comp}	Mole fractions of iron ($= 0.252$), aluminium ($= 0.623$) and zinc ($= 0.125$) in the interface compound $Fe_2Al_5Zn_x$ [18]
x_{cov}	Surface area fraction covered by crystals
x_{free}	Surface area fraction in direct contact with liquid zinc ($1 - x_{cov}$)
z	Space variable in the direction perpendicular to the plane of the sheet (m)
β	Degree of supersaturation

*Author to whom all correspondence should be addressed.

δ	Thickness of the boundary diffusion layer ($\approx$20 μm) [12]
$\Delta c_{\mathrm{Fe}}^{comp}$	Maximum difference in the concentration of iron in the intermetallic compound $Fe_2Al_5Zn_x$ (≈ -1100 mol.m^{-3}) [12, 19]
ΔG^*	Gibbs free energy of formation of a hemispherical embryo of critical size (J)
η	Dynamic viscosity of the liquid zinc (Pa·s)
ρ_{comp}	Density of $Fe_{x_{\mathrm{Fe}}^{\mathrm{comp}}}\ Al_{x_{\mathrm{Fe}}^{\mathrm{comp}}}\ Zn_{x_{\mathrm{Fe}}^{comp}}$ (4720 kg $\cdot$ m^{-3}) [12, 31]
$\sigma^{\mathrm{Zn(L)}/comp}$	Interfacial tension between interface compound and liquid zinc (J $\cdot$ m^{-2})

1. Introduction

Steel is often coated with a layer of zinc in order to protect it against corrosion. One of the most commonly used coating processes is hot dip galvanizing, frequently performed in a continuous treatment line. The steel strip is immersed in a bath of molten zinc-aluminium alloy [1, 2]. The present study considered baths containing less than 1 wt% Al, which are the most frequently employed.

In this case, two reactions occur at the interface between the steel and the liquid zinc alloy (Fig. 1), corresponding to dissolution of iron and nucleation and growth of an intermetallic phase designated $Fe_2Al_5Zn_x$ ($0 < x < 1$). The final coating is therefore composed of a thin layer of solid $Fe_2Al_5Zn_x$ about 0.1 μm thick (Fig. 2), covered with a 10 μm layer of Zn.

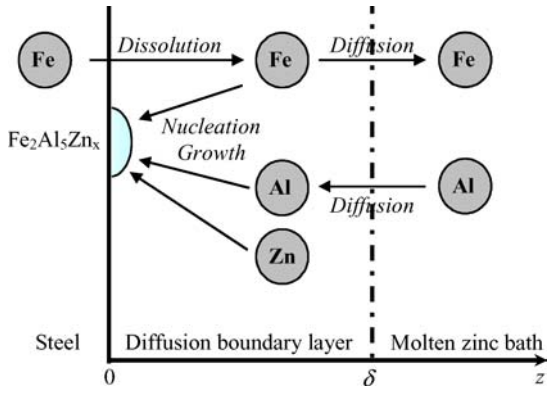

Figure 1 Schematic representation for the galvanizing reactions.

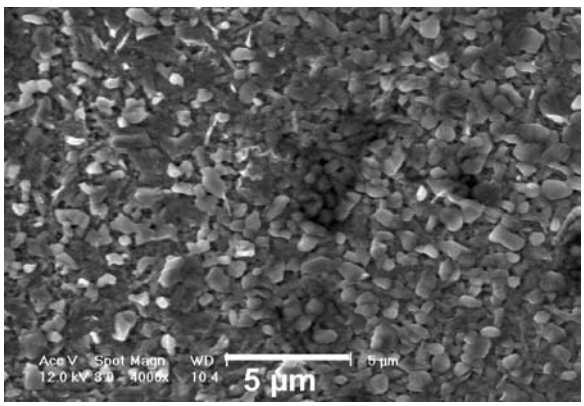

Figure 2 Layer of solid $Fe_2Al_5Zn_x$ (after selective dissolution of the layer of zinc).

Part of the iron dissolved diffuses into the bath where it contributes to the formation of $Fe_2Al_5Zn_x$ precipitates, called *dross*, about twenty microns in diameter. The liquid zinc bath thus contains 0.025 to 0.06 wt% of unwanted iron from the steel. In order to facilitate the management of industrial galvanizing baths, and in particular to limit as far as possible the formation of dross, which can cause defects in the final coating, it is necessary to be able to evaluate the variation in iron flux at the steel/zinc bath interface as a function of process parameters.

Since measurements are difficult to make in industrial plants, it has been sought to develop a model for the kinetics of the galvanizing reactions. The approach employed involved the following steps:

(1) a survey of existing models for the galvanizing process, together with published experimental data concerning growth of the intermetallic compound $Fe_2Al_5Zn_x$;
(2) construction of a model for the kinetics of the galvanizing reactions, based on the results of the literature review;
(3) validation of the model based on the experimental data available in the literature.

2. Galvanizing reactions described in the literature

The literature survey was limited to the galvanizing conditions most commonly employed (bath saturated in iron, with 0.16 to 0.2 wt% aluminium, at 450 to 480°C).

2.1. Modelling

In 1993, Linarès [3] proposed the first overall model for the galvanizing process, involving solution of the diffusion equations for iron and aluminium in the bath. The results depend on time t and on a space variable in the z direction perpendicular to the plane of the steel sheet. The boundary conditions at the steel/zinc bath interface involve the dissolution of iron according to zero order kinetics (dominant term) and growth of the intermetallic compound at the interface. In this model, growth is assumed to be limited by the diffusion of iron through the compound in the course of formation.

Subsequently, Tang [4] considered the nucleation and growth of the $Fe_2Al_5Zn_x$ intermetallic phase layer. The nucleation rate employed depends in particular on the mole fraction of aluminium at the steel/liquid zinc interface and on the number of iron atoms per unit area on the steel surface, which was considered to be equal to the number of nucleation sites. Growth was assumed to be controlled by the diffusion of aluminium in the bath.

More recently, Toussaint *et al.* [5, 6] proposed two modifications to Tang's model: (1) the nucleation rate allows for the surface roughness of the steel and the average number of iron atoms involved in the formation of an embryo; (2) growth is controlled by the diffusion of iron through the compound in the course of formation.

In conclusion, existing models for the galvanizing process do not take into account all the phenomena occurring at the steel surface; two do not consider the kinetics of iron dissolution [4, 5] and none of them allows for the growth kinetics of the $Fe_2Al_5Zn_x$ phase. In all cases, a prior assumption is made concerning the diffusion process that controls the reaction rate [3–5].

It was therefore sought to improve and complete the kinetic laws for the reactions at the steel/liquid zinc interface, for example, in order to identify the rate controlling step in the growth of the interface layer at short times.

2.2. Experimental data for the $Fe_2Al_5Zn_x$ compound formed at the interface

Numerous studies have been made on galvanized coatings to determine the nature, composition and morphology of the interface layer, including both laboratory materials [7–13] and industrial products [14–17].

These investigations reveal a thin layer of intermetallic compound, rich in iron and aluminium, which the majority of authors identify as $Fe_2Al_5Zn_x$ [7–10, 14, 15].

The precise composition of this interface layer is still the subject of controversy. For example, the measured zinc content varies in the different studies from 4 to 28 wt% for similar galvanizing conditions (0.10 to 0.23 wt% Al, temperature from 450 to 470°C) [7, 10, 11, 14, 16, 17]. Thus, since the composition of the interface layer is not accurately known, in the present work it was assumed to be uniform and equal to the composition of $Fe_2Al_5Zn_x$ in equilibrium with the galvanizing bath (20.9 wt% Zn), i.e. $x \approx 1$ [18]. The precise composition of this compound, which will be written $Fe_{x_{Fe}^{comp}}Al_{x_{Al}^{comp}}Zn_{x_{Zn}^{comp}}$ in the equations describing nucleation (Equations 6–9) and growth (Equations 11 and 14), is given in nomenclature.

The thickness of the interface layer is generally estimated from the weight of aluminium present in the compound per unit surface area ($g.m^{-2}$), for either stationary [6, 8, 9] or moving steel samples [6, 9, 17]. Using a laboratory device, Toussaint [6] showed that the growth of the interface layer is slower under turbulent conditions than in a laminar flow regime. His experimental points for the turbulent regime are in good agreement with measurements performed on industrial samples [17] and will therefore be used for validating the model (Section 4).

Recent experiments [12] have shed new light on the interface layer growth mechanisms. During the initial stages of nucleation and lateral crystal growth, a continuous layer of $Fe_2Al_5Zn_x$ compound, composed of small crystals with sizes varying from 20 to 50 nm, forms in less than a second. Growth then continues at the grain boundaries of the underlying ferrite and then in the grain centres. At the end of the galvanizing process (3 s) [8,9,12–14,16], the interface layer is composed of different colonies of crystals: (1) small equiaxed crystals with sizes ranging from 50 to 300 nm, and (2) larger elongated crystals (300 to 1000 nm) between which smaller crystals about 50 nm in diameter appear in places. The simplifying assumptions for modelling the growth will be based on these observations (Section 3.3).

3. Construction of the model for the kinetics of the galvanizing reactions

The model for the kinetics of the galvanizing reactions is based on solution of the generalized equations for the diffusion of iron and aluminium in the bath (the notation used here is defined above):

$$D_{Fe}^{Zn(L)} \frac{\partial^2 c_{Fe}}{\partial z^2} = \frac{\partial c_{Fe}}{\partial t} \tag{1}$$

$$D_{Al}^{Zn(L)} \frac{\partial^2 c_{Al}}{\partial z^2} = \frac{\partial c_{Al}}{\partial t} \tag{2}$$

With the initial and boundary conditions described below, the model enables calculation of the concentration profiles c_{Fe} and c_{Al} as a function of time t and of a space variable in the direction z perpendicular to the plane of the sheet. The value of z lies between 0, the abscissa of the interface between the steel and the liquid zinc, and δ the thickness of the boundary diffusion layer (Fig. 1). The differential equations are solved using the well-known finite difference method.

It is assumed that the diffusion coefficients for iron and aluminium in liquid zinc do not vary with concentration, since the currently available data are insufficient to define them more accurately. Furthermore, since studies of the effect of temperature on the galvanizing reactions are still rare, the analysis was essentially restricted to isothermal galvanizing conditions (the temperatures of the bath and the immersed sheet are taken to be equal).

3.1. Initial conditions

At the moment when the sheet penetrates the bath, the concentrations of iron and aluminium in the boundary diffusion layer are assumed to be constant and correspond to the composition of the liquid phase in thermodynamic equilibrium with the $Fe_2Al_5Zn_x$ surface dross [19]. The concentration of aluminium does not vary as long as nucleation has not begun:

$$\begin{aligned} c_{Fe}(z \le \delta, t = 0) &= c_{Fe}^{\circ liq} \\ c_{Al}(z \le \delta, t < t_{nucl}) &= c_{Al}^{\circ liq} \end{aligned} \tag{3}$$

3.2. Boundary conditions at the boundary diffusion layer/zinc bath interface

It is assumed that the composition of the liquid phase does not vary during galvanizing (steady state regime). The boundary conditions at the interface between the boundary diffusion layer and the molten zinc bath can therefore be written:

$$\begin{aligned} c_{Fe}(z = \delta, t) &= c_{Fe}^{\circ liq} \\ c_{Al}(z = \delta, t) &= c_{Al}^{\circ liq} \end{aligned} \tag{4}$$

3.3. Boundary conditions at the steel/liquid zinc interface

3.3.1. Before nucleation of the $Fe_2Al_5Zn_x$ compound

The dissolution of iron is the only reaction that occurs at the interface between the steel sheet and the galvanizing bath. Theoretical studies of the dissolution of a solid metal in a liquid metal always consider a first order reaction rate, falling to zero when the bath is saturated in the dissolving species [20, 21]. This approach will therefore be adopted for the dissolution of iron in liquid zinc, so that the boundary condition at the interface between the steel and the molten zinc can be written (Fig. 3a):

$$-D_{\mathrm{Fe}}^{\mathrm{Zn(L)}}\left(\frac{\partial c_{\mathrm{Fe}}}{\partial z}\right)_{z=0} = k_{diss}\left(c_{\mathrm{Fe}}^{meta}(z=0,t) - c_{\mathrm{Fe}}(z=0,t)\right) \quad (5)$$

where c_{Fe}^{meta} is the concentration of iron in the liquid zinc in metastable equilibrium with pure iron, and is calculated using the model for the Gibbs free energy of formation of the ternary liquid zinc-aluminium-iron phase described previously [22].

3.3.2. Nucleation [23]

Because of the dissolution, the concentration of iron at the interface between the steel and the liquid zinc increases and exceeds the saturation limit with respect to $\mathrm{Fe}_{x_{\mathrm{Fe}}^{comp}}\mathrm{Al}_{x_{\mathrm{Al}}^{comp}}\mathrm{Zn}_{x_{\mathrm{Zn}}^{comp}}$. The degree of supersaturation, designated β, is the driving force for heterogeneous nucleation of the intermetallic compound on the surface of the sheet, and is given by:

$$\beta = \left(\frac{a_{\mathrm{Fe}}}{a_{\mathrm{Fe}}^{sat}}\right)^{x_{\mathrm{Fe}}^{comp}} \left(\frac{a_{\mathrm{Al}}}{a_{\mathrm{Al}}^{sat}}\right)^{x_{\mathrm{Al}}^{comp}} \left(\frac{a_{\mathrm{Zn}}}{a_{\mathrm{Zn}}^{sat}}\right)^{x_{\mathrm{Zn}}^{comp}} \quad (6)$$

The determination of β involves two calculations: the composition of the bath at saturation using the equilibrium diagram [19], and the activities of iron, aluminium and zinc in the saturated and supersaturated baths, using the model for the Gibbs free energy of formation of the ternary liquid phase [22].

In agreement with theoretical and experimental studies of nucleation in liquid metals [24–27], the expression chosen for the rate of heterogeneous nucleation is as follows:

$$I = \frac{k_{nucl}}{\eta} \exp\left(-\frac{\Delta G^*}{k_B T}\right) \quad (7)$$

where ΔG^* is the Gibbs free energy of formation of a hemispherical embryo of critical radius r^*.

$$\Delta G^* = \frac{8\,\pi\, V_m^2 \left(\sigma^{\mathrm{Zn(L)}/comp}\right)^3}{3\,(k_B T \ln\beta)^2} \quad \text{and}$$

$$r^* = \frac{2\,\sigma^{\mathrm{Zn(L)}/comp} V_m}{k_B T \ln\beta} \quad (8)$$

To simplify the problem, it is assumed that nucleation and growth of the compound represent two distinct steps fully separated in time. This assumption might appear restrictive, since it neglects the growth of the first nuclei formed. In fact, it is justified by the shape of the nucleation rate curve (Equation 7). Nucleation ceases at the instant t_{nucl} when the total number of nuclei per unit surface area becomes equal to N_{nuclei} ($\approx 4.10^{14}$ m^{-2} [12]) †. The time t_{nucl} is then given by:

$$N_{nuclei} = \int_0^{t_{nucl}} I(t)\,\mathrm{d}t \quad (9)$$

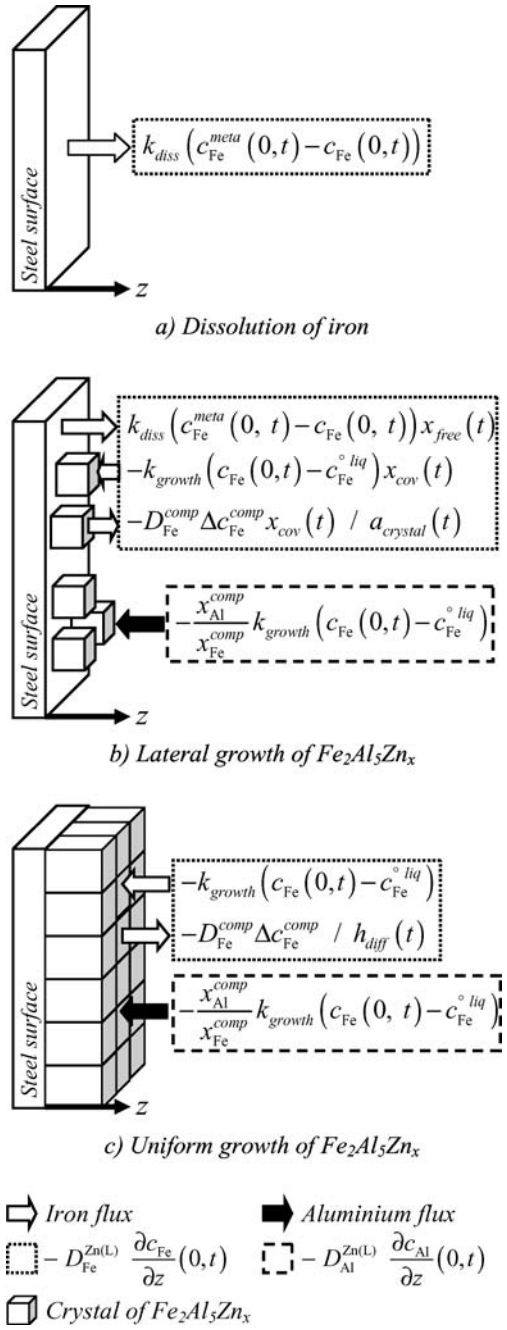

Figure 3 Schematic representation for the boundary conditions at the steel/liquid zinc interface before (3a) and after (3b, 3c) nucleation of $Fe_2Al_5Zn_x$. The crystals are assumed to grow in the form of cubes (3b) and to extend laterally until they completely cover the surface (3c).

† N_{nuclei} is estimated assuming that the surface is covered with a layer of crystals in the form of cubes of side 50 nm (first stage of lateral growth Section 2.2).

For the growth stage, as an approximation, all the hemispherical nuclei are considered to have the same size, equal to the mean critical radius r^*_{mean} of all the nuclei formed (calculated conserving n_{nucl} (mol · m^{-2}), the number of moles of intermetallic compound per unit surface area contained in the nuclei).

3.3.3. Growth

In agreement with the observations described above (Section 2.2), and introducing the simplifying assumptions to facilitate the calculations, the growth of $Fe_2Al_5Zn_x$ is assumed to occur in two steps. First of all, the crystals grow in the form of cubes of side $a_{crystal}$ and extend laterally until they completely cover the surface ($a_{crystal}$ is then equal to 50 nm). Growth then continues in a uniform manner perpendicular to the plane of the sheet. These two growth stages correspond to two different boundary conditions at the interface for iron (Fig. 3b and c):

Before the formation of a complete interface layer, the boundary condition involves (1) the iron dissolution flux from the sheet surface, in direct contact with the liquid zinc, (2) the iron flux diffusing through the crystals already formed, and (3) the iron flux consumed by growth of the crystals (Fig. 3b). Finally, at any time t,

$$\begin{aligned} -D_{\mathrm{Fe}}^{\mathrm{Zn(L)}}\left(\frac{\partial c_{\mathrm{Fe}}}{\partial z}\right)_{z=0} &= k_{diss}\left(c_{\mathrm{Fe}}^{meta}(z=0,t)-c_{\mathrm{Fe}}(z=0,t)\right)x_{free} \\ &\quad - k_{growth}\left(c_{\mathrm{Fe}}(z=0,t)-c_{\mathrm{Fe}}^{\circ\, liq}\right)x_{cov} \\ &\quad - \frac{D_{\mathrm{Fe}}^{comp}\,\Delta c_{\mathrm{Fe}}^{comp}}{a_{crystal}}\,x_{cov} \end{aligned} \tag{10}$$

The flux of iron diffusing in the intermetallic compound depends on the maximum difference $\Delta c_{\mathrm{Fe}}^{comp}$ in the concentration of iron through $Fe_2Al_5Zn_x$ [19] and on the diffusion coefficient of iron in this compound D_{Fe}^{comp} (whose estimation allows for diffusion in the grains and in the grain boundaries). The expression proposed for this flux is open to criticism since, strictly speaking, it should be based on the activities in the compound. However, considering the uncertainties in the diffusion coefficients, it remains acceptable.

In order to express the flux per unit area of iron consumed by the formation of $Fe_2Al_5Zn_x$, a first order law was chosen, taking into account the degree of saturation (to the authors knowledge, no experimental law for the growth of intermetallic compounds involving an interaction between a solid metal and a liquid metal exists).

The total quantity of compound n_{comp} (mol · m^{-2}) present on unit area of the sheet surface can be used to determine the crystal size and hence the area fraction of surface covered as a function of time t:

$$n_{comp} = n_{nucl} + \frac{k_{growth}}{x_{\mathrm{Fe}}^{comp}} \times \int_{t_{nucl}}^{t} \left(c_{\mathrm{Fe}}(z=0,t) - c_{\mathrm{Fe}}^{\circ liq}\right)dt = \frac{\rho_{comp}}{M_{comp}} N_{nuclei} a_{crystal}^3 \tag{11}$$

$$x_{cov} = a_{crystal}^2\, N_{nuclei} \quad \text{and} \quad x_{free} = 1 - x_{cov} \tag{12}$$

From the equations used for the nucleation stage (Equation 8), the initial surface area fraction covered by the crystals is $\pi\ (r^*_{mean})^2 N_{nuclei}$.

The crystals meet in the first layer when $x_{cov} = 1$ (Fig. 3c). The thickness of the interface layer is then h_{diff} and the boundary condition for any time t is given by:

$$-D_{\mathrm{Fe}}^{\mathrm{Zn(L)}}\left(\frac{\partial c_{\mathrm{Fe}}}{\partial z}\right)_{z=0} = -\frac{D_{\mathrm{Fe}}^{comp}\,\Delta c_{\mathrm{Fe}}^{comp}}{h_{diff}} - k_{growth}\left(c_{\mathrm{Fe}}(z=0,t) - c_{\mathrm{Fe}}^{\circ\, liq}\right) \tag{13}$$

The diffusion of aluminium in the interface layer already formed is neglected. During growth of the compound, the boundary condition for aluminium at the interface therefore depends only on the aluminium flux necessary to form the compound (Fig. 3b and c), so that for any time t:

$$D_{\mathrm{Al}}^{\mathrm{Zn(L)}}\left(\frac{\partial c_{\mathrm{Al}}}{\partial z}\right)_{z=0} = \frac{x_{\mathrm{Al}}^{comp}}{x_{\mathrm{Fe}}^{comp}} k_{growth}\left(c_{\mathrm{Fe}}(z=0,t) - c_{\mathrm{Al}}^{\circ\, liq}\right) \tag{14}$$

4. Predictions of the galvanizing kinetics model

The model was applied to galvanizing in a bath containing 0.2 wt% aluminium and saturated in iron (T = 460°C).

Four physical parameters involved in the model were unable to be determined accurately, i.e., $D_{\mathrm{Al}}^{\mathrm{Zn(L)}}$, k_{diss}, k_{growth}, $\sigma^{\mathrm{Zn(L)}/comp}$. These parameters were adjusted, starting from an initial estimation [12], by comparing the results of the calculation with Toussaint's experimental measurements [6]. The values obtained in this way are: $D_{\mathrm{Al}}^{\mathrm{Zn(L)}} = 5.0 \cdot 10^{-9}$ m^2 · s^{-1}, $k_{diss} = 1.7 \cdot 10^{-5}$ m · s^{-1}, $k_{growth} = 1.7 \cdot 10^{-4}$ m · s^{-1}, $\sigma^{\mathrm{Zn(L)}/comp} = 0.245$ J · m^{-2}.

Fig. 4 shows the weight of aluminium per unit area of intermetallic compound on the surface as a function of galvanizing time. After an incubation period corresponding to the establishment of the supersaturation β, the compound growth rate is very rapid, but slows significantly after 0.4 s of immersion (growth is then controlled by the diffusion of iron through the compound). The calculation is in good agreement with Toussaint's experimental points [6]. The differences between the experimental points and the calculation at the shortest contact times can be the result of both causes: (1) Toussaint's experimental measurements at 0.1 s are probably

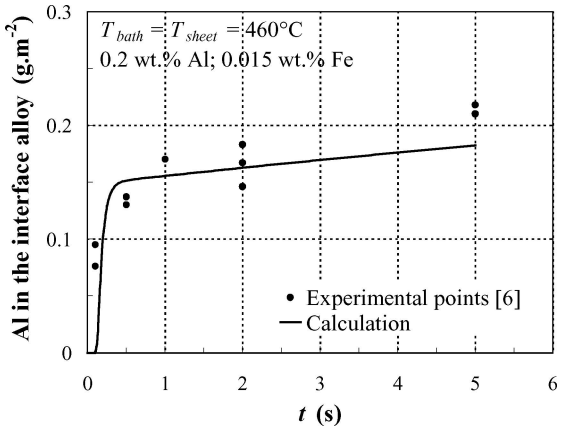

Figure 4 Weight of aluminium per unit area of interface compound on the surface as a function of galvanizing time: The calculation is in good agreement with Toussaint's experimental points [6].

overestimated, due to the cooling time of his samples, during which the interfacial layer is likely to grow, and (2) the calculation could be underestimated because some parameters of the model are not well-known.

The model is capable of calculating the following parameters as a function of time: the concentration profiles for iron and aluminium in the boundary diffusion layer, the nucleation rate, the time t_{nucl} (= 0.09 s), the average critical embryo radius ($r^*_{mean} = 0.82$ nm), the degree of supersaturation β (= 2.3) and the time necessary to form a continuous layer (= 0.2 s).

The calculation program also predicts the right order of magnitude for the weight of iron dissolved, albeit slightly overestimated (0.3 g · m^{-2} after 3 s, compared to 0.2 g · m^{-2} [28]).

5. Conclusions

A model has been developed to describe the kinetics of galvanizing reactions that occur at the steel/liquid zinc interface (dissolution of iron, heterogeneous nucleation and growth of the intermetallic phase designated $Fe_2Al_5Zn_x$). The model has been validated using experimental data available in the literature for a three-second galvanizing treatment.

The model is capable of calculating the following parameters as a function of time: the concentration profiles for iron and aluminium in the boundary diffusion layer, the nucleation rate, the average critical embryo radius, the establishment of supersaturation and the time necessary to form a continuous layer.

More results and a study of the sensitivity of the model to variations of four important physical parameters involved in the model ($D_{\mathrm{Al}}^{\mathrm{Zn(L)}}$, k_{diss}, k_{growth}, $\sigma^{\mathrm{Zn(L)}/comp}$) will be given elsewhere.

Acknowledgments

The authors are extremely grateful to Dr. M. Guttmann et Dr. P. Drillet for their enthusiasm and help with this study.

References

1. M. GUTTMANN, *Mater. Sci. Forum* **155/156** (1994) 527.
2. A. R. MARDER, *Progr. Mater. Sci.* **45** (2000) 191.
3. I. LINARÈS, "Modélisation du réacteur de galvanisation en continu", PhD thesis, École Centrale Paris (1993).
4. N. Y. TANG, *Metallurg. Mater. Trans. A* **26A** (1995) 1699.
5. P. TOUSSAINT, L. SEGERS, R. WINAND and M. DUBOIS, *ISIJ Intern.* **38** (1998) 985.
6. P. TOUSSAINT, "Contribution à l'ètude de la formation de la couche d'inhibition de l'acier galvanisé en continu", PhD thesis, Université Libre de Bruxelles (1997).
7. Y. LEPRÊTRE, "Étude des mécanismes réactionnels de la galvanisation", PhD thesis, Université Paris XI Orsay (1996).
8. N. Y. TANG and G. R. ADAM, in "The Physical Metallurgy of Zinc Coated Steel", edited by A. R. Marder (The Minerals, Metals and Materials Society, 1993) p. 41.
9. J. FADERL, W. MASCHEK and J. STRUTZENBERG, in Proceedings of the Third International Conference on Zinc and Zinc Alloy Coated Steel Sheet (Galvatech'95) (The Iron and Steel Society, Warrendale, PA, 1995) p. 675.
10. E. BARIL and G. L'ESPÉRANCE, *Metallurg. Mater. Trans. A* **30A** (1999) 681.
11. S. E. PRICE, V. RANDLE, M. PICHILINGI and T. MAYES, *La revue de Métallurgie—CIT* **96** (1999) 381.
12. M.-L. GIORGI, "Étude des cinétiques des réactions de galvanisation", PhD thesis, École Centrale Paris (2000).
13. I. HERTVELDT, L. VANDENBERGHE and B. C. DE COOMAN, in Proceedings of the Fourth International Conference on Zinc and Zinc Alloy Coated Steel Sheet (Galvatech'98) (The Iron and Steel Institute of Japan, 1998) p. 190.
14. G. J. HARVEY and P. D. MERCER, *Metallur. Trans.* **4** (1973) 619.
15. J. FADERL, M. PIMMINGER and L. SCHÖNBERGER, in Proceedings of the Second International Conference on Zinc and Zinc Alloy Coated Steel Sheet (Galvatech'92), edited by CRM (Verlag Stahleisen GmbH, Düsseldorf, Germany, 1992) p. 194.
16. E. McDEVITT, Y. MORIMOTO and M. MESHII, *ISIJ Intern.* **37** (1997) 776.
17. M. GAGNÉ, E. BARIL, S. BÉLISLE, G. L'ESPÉRANCE, E. BOUTIN, B. HONG and F. GOODWIN, in "Zinc-Based Steel Coating Systems: Production and Performance", edited par F. E. Goodwin (The Minerals, Metals and Materials Society, 1998) p. 229.
18. Z. W. CHEN, R. M. SHARP and J. T. GREGORY, Mater. Sci. Tech. **6** (1990) 1173.
19. N.-Y. TANG, *J. Phase Equil.* **21** (2000) 70.
20. E. A. MOELWYN-HUGUES, "The Kinetics of Reactions in Solution", 2nd ed. (Clarendon Press, Oxford, 1947) p. 374.
21. J. M. LOMMEL and B. CHALMERS, *Trans. Metallur. Soc. AIME* **215** (1959) 499.
22. M.-L. GIORGI, J.-B. GUILLOT and R. NICOLLE, *Calphad* **25** (2001) 461.
23. A. S. MYERSON and R. GINDE, "Handbook of Industrial Crystallization" (Butterworth-Heinemann Series in Chemical Engineering, 1993) p. 33.
24. D. TURNBULL, *Contempor. Phys.* **10** (1969) 473.
25. J .W. CHRISTIAN, "The Theory of Transformations in Metals and Alloys—Part 1 Equilibrium and General Kinetic Theory," 2nd edn. (Pergamon Press, 1975) p. 418.
26. C. V. THOMPSON and F. SPAEPEN, *Acta Metallurgica* **31** (1983) 2021.
27. X. ZHANG, *ibid.* **46** (1998) 1135.
28. A. GAST-BRAY, P. DURIGHELLO, T. MOREAU, I. LINARÈS and J. P. SPILL, Private communication, 1995.
29. L. N. LARIKOV, *Avt. Svarka* **5** (1968) 68.
30. M.-L. GIORGI, P. DURIGHELLO, R. NICOLLE and J.-B. GUILLOT, *J. Mater. Sci.* **39** (2004) 5803–5808.
31. Z. W. CHEN, R. M. SHARP and J. T. GREGORY, *Mater. Forum* **14** (1990) 130.

Received 31 March
and accepted 20 October 2004